

High-yielding aquifers in crystalline basement: insights about the role of fault zones, exemplified by Armorican Massif, France

Journal Article**Author(s):**

Roques, Clément; Bour, Olivier; Aquilina, Luc; Dewandel, Benoît

Publication date:

2016-12

Permanent link:

<https://doi.org/10.3929/ethz-b-000119669>


Rights / license:

[In Copyright - Non-Commercial Use Permitted](#)

Originally published in:

Hydrogeology Journal 24(8), <https://doi.org/10.1007/s10040-016-1451-6>

High-yielding aquifers in crystalline basement: insights about the role of fault zones, exemplified by Armorican Massif, France

Clément Roques^{1,2}  · Olivier Bour¹ · Luc Aquilina¹ · Benoît Dewandel³

Received: 24 November 2015 / Accepted: 14 July 2016 / Published online: 15 August 2016
© Springer-Verlag Berlin Heidelberg 2016

Abstract While groundwater constitutes a crucial resource in many crystalline-rock regions worldwide, well-yield conditions are highly variable and barely understood. Nevertheless, it is well known that fault zones may have the capacity to ensure sustainable yield in crystalline media, but there are only a few and disparate examples in the literature that describe high-yield conditions related to fault zones in crystalline rock basements. By investigating structural and hydraulic properties of remarkable yielding sites identified in the Armorican Massif, western France, this study discusses the main factors that may explain such exceptional hydrogeological properties. Twenty-three sites, identified through analysis of databases available for the region, are investigated. Results show that: (1) the highly transmissive fractures are related to fault zones which ensure the main water inflow in the pumped wells; (2) the probability of intersecting such transmissive fault zones does not vary significantly with depth, at least within the range investigated in this study (0–200 m); and (3) high yield is mainly controlled by the structural features of the fault zones, in particular the fault dip and the presence of a connected storage reservoir. Conceptual models that summarize the hydrological properties of high-yield groundwater resources related to fault zones in crystalline basement are shown and discussed.

Keywords Crystalline rocks · Fault zone · Hydraulic properties · Well yield · France

Introduction

One third of the continental crust surface is composed of igneous and metamorphic rocks (Amiotte Suchet et al. 2003; Blatt and Jones 1975). Groundwater in crystalline rocks constitutes a crucial resource for highly populated zones worldwide, supplying drinking water as well as industrial and farming activities (Gleeson et al. 2012). Due to the heterogeneity of crystalline rock aquifers and because of the absence of information on sustainable yield conditions, resource availability is difficult to evaluate and often under-estimated (Banks 1998; Mabee 1999).

The hydraulic properties of crystalline rocks often result in a poorly productive resource. Their ability to conduct water is mainly controlled by the density of fractures affecting the rock massif as well as their aperture and connectivity at the watershed scale (Berkowitz 2002; Stober and Bucher 2006). Average permeability values encountered in crystalline basement range typically from 10^{-15} to 10^{-17} m² (Gleeson et al. 2011; Ranjram et al. 2015; Stober and Bucher 2014). Conceptual models regarding structural context and hydraulic properties of the first tens of meters of the crystalline basement have been widely discussed through descriptive and experimental studies worldwide (Anderson 2015; Banks et al. 2002, 2009; Boutt et al. 2010; Dewandel et al. 2006; Hencher et al. 2011; Maréchal et al. 2004; St. Clair et al. 2015; Stober and Bucher 2006; Welch and Allen 2014; Wyns et al. 2004). These models mainly highlight that: (1) the density of permeable fractures decreases rapidly with depth due to overburden stress, (2) aquifers are often restricted to the upper 50 m where jointing and, in some regions, weathering processes may provide a good connectivity at the watershed scale (Dewandel

✉ Clément Roques
clement.roques@erdw.ethz.ch; roquesclm@gmail.com

¹ OSUR Research Federation – Géosciences, UMR 6118, University of Rennes 1, CNRS, Av. du Général Leclercq, 35 042 Rennes, France

² Department of Earth Sciences, ETH Zürich, Building NO, Office G5, Sonneggstrasse 5, 8092 Zürich, Switzerland

³ BRGM, Water Dept (D3E) – New Water Resource & Economy Unit, 1039 rue de Pinville, 34000 Montpellier, France

et al. 2012; Guihéneuf et al. 2014) and (3) these superficial aquifers generally ensure a limited resource only, of a few cubic-meters per hour and per well.

It is well known that fault zones may provide significant groundwater resources in crystalline rocks (Bense et al. 2013; Caine et al. 1996); nevertheless, the hydraulic properties of fault zones are highly variable. They depend on remote stresses, type of displacement, age and lithology (Bense et al. 2013; Caine et al. 1996). Low-permeability fault zones in crystalline media, where described, act as barriers to groundwater flow (Gleeson and Novakowski 2009; Malgrange and Gleeson 2014), while high transmissive and productive structures have also been characterized (Henriksen 2003; Le Borgne et al. 2007; Neves and Morales 2006; Roques et al. 2014b; Seebeck et al. 2014). Beyond the intrinsic variability of fractured media, it remains unclear whether the latter examples should be considered as exceptional case studies or if the role of fault zones may be of interest for groundwater abstraction at the regional scale. To bring new insights on groundwater resources in crystalline rocks, this study examines the potential for high yield in the Armorican Massif (Brittany, Western France, Fig. 1), a crystalline basement where sub-surface groundwater resources have been intensely investigated.

This study explores structural and hydrogeological conditions that may lead to high-yield resources. By analyzing data available for the Armorican Massif, the role of fault zones for

development of a sustainable resource is discussed. The main objective is to give characteristic features of high-yield conditions in a regional-scale framework, by investigating (1) the distribution of hydraulic properties of high-yielding sites, (2) the geological and structural conditions that may lead to these yield conditions and (3) the resource sustainability under pumping conditions for identified structures.

Context

Geological context

The Armorican Massif is mainly composed of plutonic and metamorphic rocks (Fig. 1) that were formed during the Cadomian and Hercynian orogenies (Ballèvre et al. 2009; Chantraine et al. 2001; Guillocheau et al. 2003). Two major shear zones, known as the North and South Armoricain Shear Zones (Fig. 1, NASZ and SASZ, respectively) cross the region. During the Meso-Cenozoic era, the Armorican Massif was subjected to compressive tectonic phases induced by the collision between Europe and Africa. This event was responsible for the formation of large-scale NNW–SSE fault systems (Fig. 1) known as the Quessoy Nort-Sur-Erdre (QFZ), Kerforne (KFS) and Mayenne (MFZ) faults (Bonnet et al. 2000; Guillocheau et al. 2003; Van Vliet-Lanoë et al. 1997).

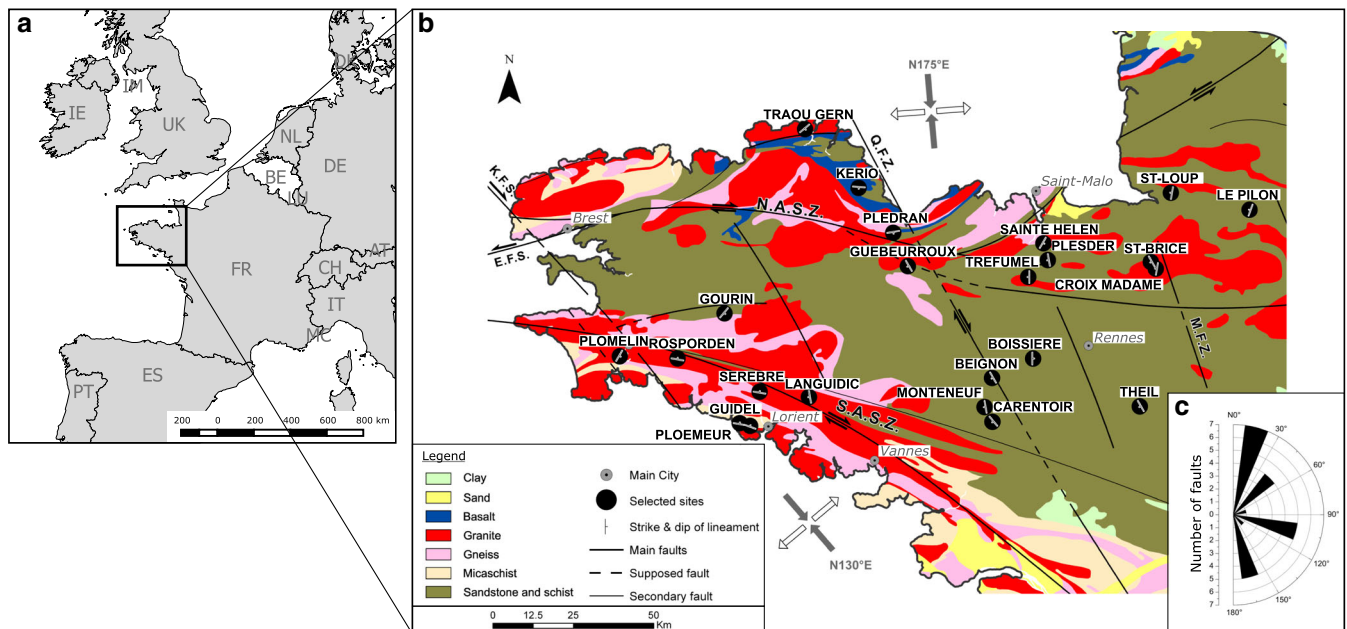


Fig. 1 a Location map of the Armorican Massif (Brittany, France). b Geological map and location of the selected sites. The map displays the main lithological units. The regional stress field is represented, with grey arrows indicating the direction of the maximum compression σ_1 and white arrows the direction of the minimum horizontal stress σ_2 —from Mazabraud et al. (2004, 2005). The main regional faults are also represented: NASZ North Armoricain Shear Zone, SASZ South

Armoricain Shear zone, QFZ Quessoy-Nord/Sur-Erdre Fault zone, MFZ Mayenne Fault System, KFS Kerforne Fault System and EFS Elorne Fault System—from Van Vliet-Lanoë et al. (1997). FR France; adjacent countries: ES Spain, IT Italy, CH Switzerland, BE Belgium, LU Luxembourg, DE Germany. c Rose diagram of fault zones distribution showing the main structural orientations of the selected sites

Water supply strategy

The Armorican Massif is under a temperate climate with an average yearly amount of precipitation around 1,000 mm. Surface water provides 75 % of the drinking supply in the region, whereas groundwater accounts for only 25 % according to the French Water Agency (Agence de l'eau Loire-Bretagne 2016). The French Water Agency references around 400 sites in which groundwater is extracted for water supply within the Armorican Massif. In all, 40 % of the groundwater supply comes from crystalline rock aquifers, while the remaining is ensured by alluvial, sedimentary and volcanic aquifers (Fig. 1). Historically, groundwater sites located in the crystalline basement mainly consisted of several sub-surface wells (20–30 m depth) drilled in the very first part of the basement where regolith and shallow fractured rocks were sufficiently developed. Such a context allowed a sufficient cumulated flow to secure local water needs in poorly productive areas. During the last few decades, deeper wells in the basement (>50 m depth) have been installed to meet the increasing water demand, as well to avoid recurrent problems of surface water contamination. At the regional scale, the average borehole flow rate in the crystalline basement is estimated to be around 9 m³/h (Mougin et al. 2008).

Methodology

Description of databases

Highly productive groundwater sites in the Armorican crystalline basement were identified by cross-analyzing two available databases. The first one concerns geological maps and borehole data archives (BSS, Base de Données du Sous-Sol) provided by the French Geological Survey (BRGM), with information from almost 12,000 wells in the crystalline basement of the Armorican Massif (data available through the BRGM website, BRGM 2016). Among geological maps and well locations, the BSS also includes, when available, technical and geological logs of the wells, airlift flow-rate profile data, and sometimes pumping test data, as well as technical reports from drilling and engineering offices. The second one, the French Water Agency database, compiles information regarding water supply in France. Particularly, it provides the annual volume extracted from the 400 groundwater sites in the Armorican crystalline basement operated for water supply (data available through the French Water Agency website, Agence de l'eau Loire-Bretagne 2016).

Sites selection

The specific sites investigated in this study have been selected based on well yield but also data availability. In a

first step, high-yielding boreholes were selected based on borehole flow rate estimated from airlift measurements available in the BSS. Most boreholes of the database are poorly productive, the average flow rate being around of 9 m³/h (Mougin et al. 2008 and see section 'Hydraulic properties of fault zones'). In this study, a minimum of 40 m³/h of borehole flow rate, e.g. 4 times the average, is considered to be a reliable quantity to define a high-yielding well. This first selection resulted in the identification of 314 wells, which represent 2.5 % of the total number of wells that are referenced in the BSS.

In a second step, some sites were disregarded on the basis of available geological and hydrogeological information. Two criteria were determinant in this second step: (1) the information on depth-variation of airlift flow rate and (2) the evaluation of aquifer transmissivity through pumping test data. Those information were extracted, when available, directly from the BSS or were collected by contacting the engineering offices that were in charge of the borehole drilling and testing.

In a final step, the annual volume of water extracted from the selected sites was obtained from the Water Agency database when the site was used for water supply. In the end, a total number of 74 boreholes ranging from 50 to 220 m depth were selected within 23 groundwater abstraction sites, which represents about 25 % of the whole database regarding wells displaying yield of more than 40 m³/h (Table 1).

Data analysis

Borehole transmissivity

Borehole transmissivity (T_b) was estimated by engineering offices by modeling the drawdown evolution during pumping tests using Theis equations (Theis 1935). Although this solution does not take into account the complex flow behavior that may be involved in fractured and compartmentalized reservoirs (Butler and Liu 1991; Dewandel et al. 2014; Meier et al. 1998), the Theis solution is generally chosen by engineering offices because it provides first-order estimates of the aquifer hydraulic properties. Borehole transmissivities were estimated by fitting the Theis solution on the late drawdown signal. The drawdown in compartmentalized media tend to follow a Theis-type response at late time—a straight line in a semi-logarithmic plot (Renard et al. 2008)—which corresponds to the transmissivity of the main storage reservoir present in the aquifer (Dewandel et al. 2014; Meier et al. 1998).

Airlift flowrate and fracture transmissivities

The variations in airlift flow measurements with depth were investigated based on available engineering and drilling reports. Airlift tests are classically carried out during or after

Table 1 Characteristics of the selected sites. *asl* above sea level; *gbs* below ground surface

Name	X_LAMB93 [m]	Y_LAMB93 [m]	Elevation [m asl]	No. of boreholes	Depth [m]	Slotted interval [m bgs]	Geology	Depth of the water level [m bgs]	Transmissivity (pumped borehole) [m ² /h]	Airift Flowrate [m ³ /h]	Operating Flowrate [m ³ /day]
Pledran	275,099	6,833,973	81	6	80	31–71	Brioverian schist	1.52	2.52	61	740
Kerio	261,507	6,851,664	93	5	100	24–104	Brioverian schist	3.98	0.94	41	600
Guebeuroux	280,846	6,820,863	210	1	120	30–104	Hercynian granite	1	2.52	90	600
Traou Gern	240,455	6,874,788	42	5	100	29–95	Hercynian gneiss	5	3.60	114	2,000
Sainte Helen	334,103	6,829,844	43	5	80	Open	Cadomian gneiss	Artesian	6.12	101	1,400
Trefumel	328,166	6,816,603	29	3	130	Open	Brioverian schist	5.9	3.96	40	600
Plomelin	167,704	6,785,532	25	1	130	59–98	Hercynian granite	1.02	3.96	50	600
Rosporden	190,406	6,784,665	115	2	200	33–111	Hercynian granite	7.19	0.63	42	1,000
Boissière	330,068	6,784,630	55	1	100	Open	Brioverian schist	Artesian	2.15	50	400
Plesder	335,834	6,823,264	59	5	120	25–122	Brioverian schist	5.87	0.94	41	500
Theil	371,972	6,765,829	70	3	100	26–81	Brioverian schist	14.29	2.18	61	–
St+Brice en Coglès	376,274	6,822,556	91	3	250	28–60-open	Brioverian schist	5	2.52	103	600
Croix Madame	378,241	6,819,881	107	3	150	Open	Cadomian granite	0.5	1.80	67	600
Le Pilon	415,081	6,843,060	185	1	100	26–68	Brioverian schist	8.88	0.66	95	1,000
Saint-Loup	384,207	6,849,740	70	2	100	23–63	Brioverian schist	4.50	4.32	145	1,000
Beignon	313,927	6,776,994	92	4	100	65–95	Brioverian schist	Artesian	7.67	89	2,500
Carentoir	314,088	6,759,747	37	3	135	68.127	Brioverian schist	1.70	2.56	76	1,200
Serebre	222,622	6,771,550	25	2	150	79–169	Hercynian granite	6.74	7.92	68	1,600
Gourin	208,846	6,802,281	151	4	80	Open	Brioverian schist	7.59	1.80	66	500
Guidel	214,798	6,759,202	10	6	130	37–92	Hercynian schist	Artesian	2.56	150	1,500
Languidic	241,995	6,769,503	80	1	150	Open	Brioverian schist	0.91	1.44	53	500
Monteneuf	310,971	6,765,547	103	4	100	Open	Brioverian schist	35.85	8.28	105	500
Kermadaye-Plomeur	218,897	6,758,130	24	4	70	45–70	Hercynian schist	5	7.92	78	1,500

drilling to lift sand and particles from the borehole, but they also are done to provide an evaluation of the well yield and the location of productive zones. These data can also be used to estimate inflow rates. The values of inflow rate extracted from airlift measurement presents clear uncertainties but are often used as a first estimation of borehole and fracture flow properties. The relative uncertainty in the estimation of fracture flow rate is around 10 %. The depth of the major inflows was referenced to the regolith depth, i.e. the transition between unconsolidated sandy-clay materials and unweathered rock, which is easily identified during drilling. This provided a common reference for depth variations, independent of the regolith thickness (Ayraud et al. 2008; Dewandel et al. 2006; Maréchal et al. 2004).

In order to estimate fracture transmissivities (T_f), the contribution of each fracture to the total borehole flow rate was computed based on the airlift profiles, assuming that the fracture flow rate was in quasi-steady state condition during measurements. The fracture transmissivity is simply estimated by multiplying the flow contribution to the borehole transmissivity T_b (Kabala 1994; Paillet 1998). Figure 2 summarizes the methodology used to compute the fracture transmissivities.

Fault zone productivity

The productivity for each pumping site may be quantified through different ways. The first one may be simply based on the average operating flow rate given by the French Water Agency. Nevertheless, this value mainly depends on local water needs and is not necessarily representative of the site hydrogeological properties. For this reason, the degree of

productivity of each site was examined by estimating the specific capacity (SC [(m³/h)/m]) from the available pumping data:

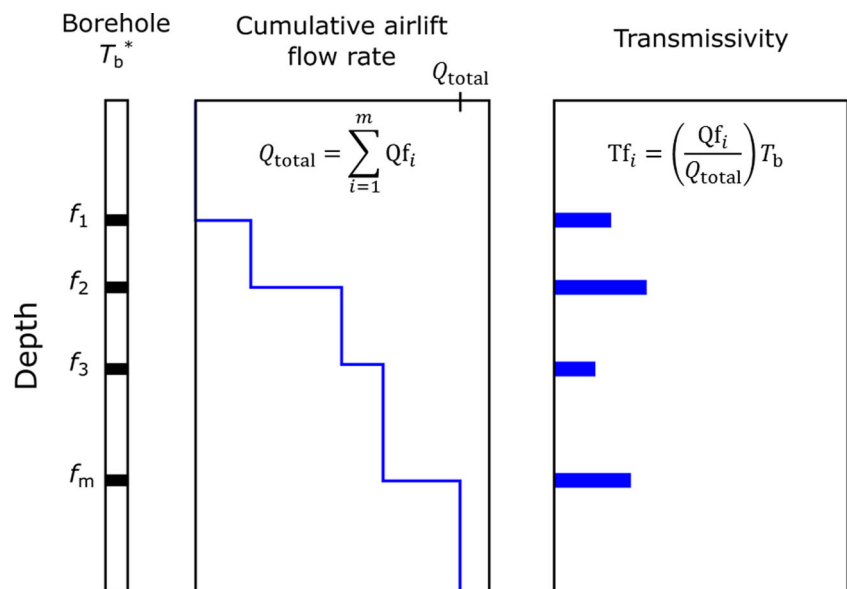
$$SC = Q / s_w \tag{1}$$

which corresponds to the pumped flow rate (Q) normalized by the corresponding drawdown (s_w) at steady state. The specific capacity is commonly used to estimate well yield, by providing the amount of flow mobilized by the aquifer per unit of draw-down (Boutt et al. 2010; Dewandel et al. 2012; Razack and Lasm 2006; Srivastav et al. 2007). The specific capacity is directly related to aquifer properties (transmissivity T , storage coefficient S) by the Cooper and Jacob approximation of the Theis equation (Singhal and Gupta 2010):

$$SC = Q / s_w \sim \frac{T_b}{0.183 \log\left(\frac{2.25 T_b t}{r_w^2 S}\right)} \tag{2}$$

where r_w is the well radius and t is the time of pumping. According to Eq. (2), the specific capacity decreases with time of pumping. In order to define a common approach for comparing the specific capacity for each of the selected sites for which unequal pumping tests data are available—i.e. duration of the test from 1 h to several months—a common reference was chosen: drawdown (s_w) was taken after 1 h of pumping (Q), which corresponds to the minimum duration of pumping tests in the dataset. It is commonly assumed that the drawdown is mainly controlled by the aquifer properties after 1 h of pumping and it is less influenced by the well itself. In the sites for which longer pumping tests have been carried out, a statistical analysis is used in order to appreciate the sensitivity of the specific capacity with time of pumping (see section

Fig. 2 Methodology employed to compute the fracture transmissivity based on airlift flow measurement and borehole transmissivity. Q_{total} is the cumulated airlift flow rate, Qf_i and Tf_i are respectively the airlift flow rate and the fracture transmissivity corresponding to fracture f_i , with $i = 1, 2, \dots, m$. T_b is the borehole transmissivity estimated from pumping test interpretation



(* T_b : borehole transmissivity estimated from pumping test interpretation)

‘Productivity of the aquifer’). In order to compare the pumping curves, time were re-normalized according to the variation of flow rate during the test (Bourdet and Ayoub 1989).

Additionally, in order to describe transitory flow behaviors, diagnostic plots were analyzed, which included plotting the logarithmic derivative of the specific drawdown (inverse of the specific capacity), $\partial(s_w/Q)/\partial[\ln(t)] = \partial \ln(t)$, as a function of time in the log-log scale. This graphical method is classically used to describe specific flow conditions involved during the transitory times of pumping and identify appropriate conceptual models of the aquifer (Renard et al. 2008).

Results

Hydraulic properties of fault zones

The potential in terms of groundwater abstraction of the 23 selected sites represents around 8–10 million m^3/year . This volume is approximately 2.5 % of the total annual volume used for drinking water (considering surface water and groundwater) in the Armorican Massif, which is about 315 million m^3/year on average estimated on 2008–2011 data (data available through the French Water Agency website, Agence de l’eau Loire-Bretagne 2016) and 25 % when only considering the total volume extracted from bedrock aquifers (30 million m^3/year). Thus, although not representative of the whole database (Fig. 3a), the sites selected in this study

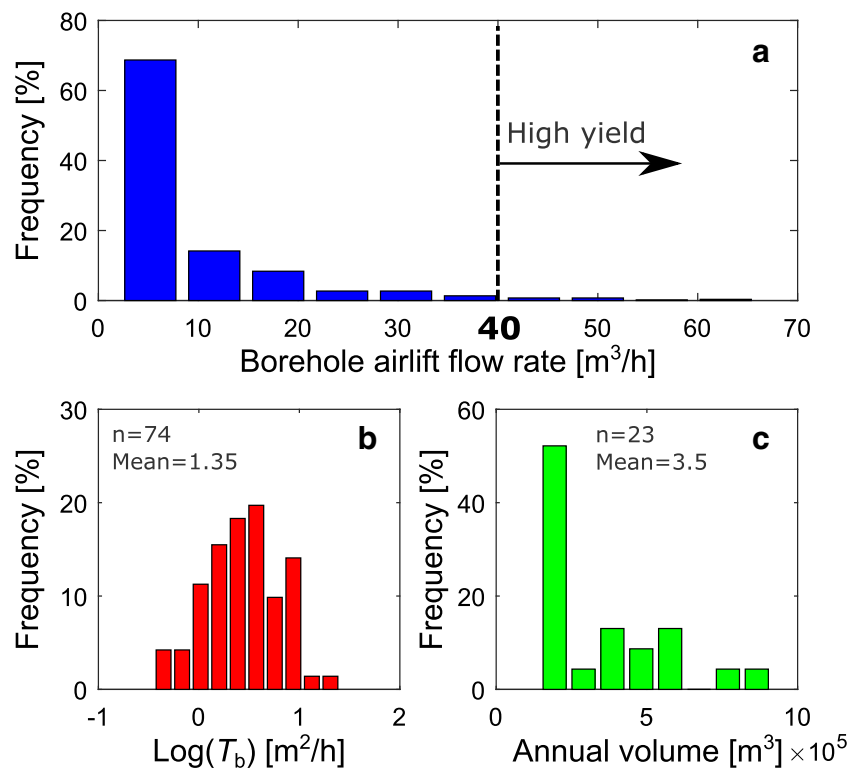
represent a significant contribution in terms of groundwater abstraction in the bedrock aquifers of the Armorican Massif.

The distribution of the borehole transmissivity (T_b) deduced from pumping test interpretations is displayed in Fig. 3b. It shows a log-normal distribution with remarkably higher values than classically described in crystalline rocks (Chilton and Foster 1995; Singhal and Gupta 2010; Taylor and Howard 2002). The average transmissivity in this dataset is $2.88 \text{ m}^2/\text{h}$ ($8 \times 10^{-4} \text{ m}^2/\text{s}$) with a maximum of $25.2 \text{ m}^2/\text{h}$ ($7 \times 10^{-3} \text{ m}^2/\text{s}$).

Airlift flow measurements are displayed in Fig. 4a,b. In total, 529 permeable major inflows were identified within the 74 boreholes. Fracture flow distribution shows high values with an average of $12 \text{ m}^3/\text{h}$ and a maximum of $220 \text{ m}^3/\text{h}$. The fracture transmissivity values deduced from the airlift profiles also follow a well-defined log-normal distribution (Fig. 4c,d), centered on $\log(T_f) = 0.25 \text{ m}^2/\text{h}$ ($5.6 \times 10^{-5} \text{ m}^2/\text{s}$). Although only highly productive groundwater sites were selected in this study, the standard deviation is relatively large with data distributed over three orders of magnitude. On average, seven transmissive fractures were identified for each borehole. Each borehole presents a major inflow zone, which ensures more than 50 % of the total borehole transmissivity, regardless of depth. This zone typically consists of one to three main inflows and corresponds to the main transmissive fault zone.

In order to analyze the depth variation of the hydraulic properties within this dataset, the fracture density as well as the average transmissivity and its distribution (range between first and third quartile) were computed for each 10-m interval. Results are

Fig. 3 **a** Borehole flow rate distribution for crystalline aquifers in the Armorican Massif. **b** Transmissivity distribution for the 23 selected sites with high flow rate ($\geq 40 \text{ m}^3/\text{h}$; 74 boreholes) and **c** global groundwater extraction from the 23 selected sites



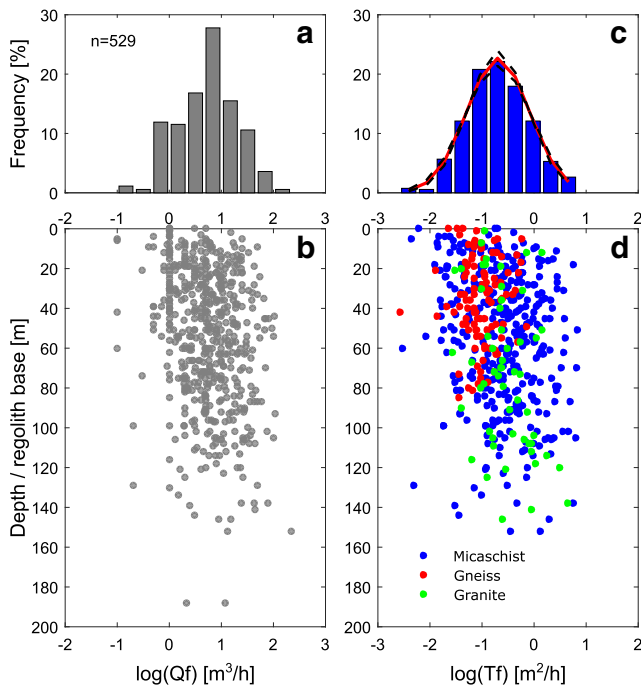


Fig. 4 **a** Histogram of fracture flow rates. **b** Fracture flow rate along depth below regolith. **c** Histogram of fracture transmissivities (T) investigated in this study along with a log normal fit. **d** Fracture transmissivity vs. depth below regolith (the *color* differentiates the rock lithology)

represented in Fig. 5a,b. The transmissive fracture density exhibits little variation with depth. Fewer numbers of transmissive fractures were observed between 130 and 160 m below the regolith layer, but these depths also correspond to a smaller number of measurements. Only 30 % of the boreholes reach

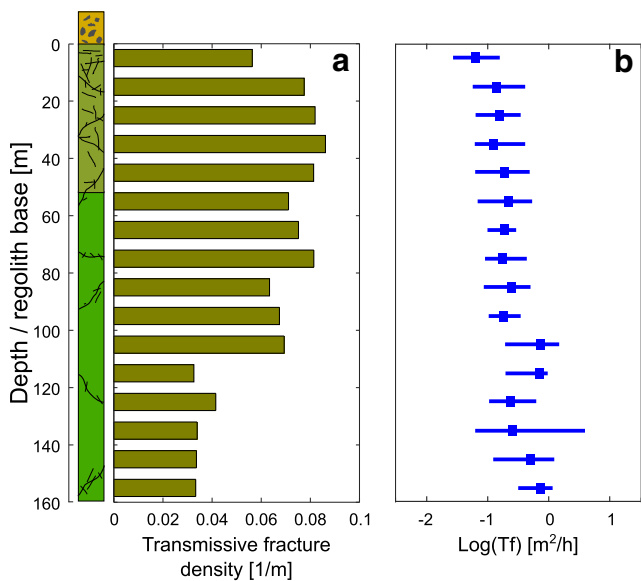


Fig. 5 **a** Transmissive fracture density per meter computed over an interval length of 10 m. **b** Median (*blue squares*) depth evolution of fracture transmissivity computed over a 10-m depth interval. *Bars* represent the range between the 1st and 3rd quartiles

130-m depth. The results also show that, for the depth-range investigated in this study, the average fracture transmissivity does not seem to be directly dependent on the depth. Despite the limited number of observation wells deeper than 130 m, the maximum average values were computed for the 100–160-m interval. Thus, highly transmissive fault zones can be found even at relatively great depth, largely below the regolith layer.

Location and structural settings

The 23 selected sites are located on Fig. 1, which displays the main lithological units and major regional faults of the Armorican Massif. All the sites are situated in areas of low topography between 20 and 100 m above sea level, the maximum elevation of the Armorican Massif being around 400 m. Altogether, 70 % of the productive sites were found in schist or micaschist formations, 20 % in granite and 10 % percent in gneiss formations. Because schists are more represented in the Armorican Massif compared to others lithological units, those numbers do not highlight a direct influence of the lithology on borehole productivity.

The selected sites appear to be located near a main fault either already well known from geological maps or identified through lineaments analysis. In some sites, additional geological information was compiled from core analysis and subsurface geophysical investigations, which allows the estimation of the orientation of the major fault zone as well as providing a rough estimate about the dip of the fault zones (Fig. 1).

In some areas, the high-yielding fault zones are well correlated to the orientation of regional tectonic-fault systems (Fig. 1). South of South Armorican Shear Zone (SASZ), most of the productive fault zones are oriented NW–SE, sub-parallel to the SASZ. In the central domain, the productive fault zones follow a N150°E or N–S orientation, sub-parallel to the Quessoy-Nord/Erdre Fault Zone (QFZ) and the Mayenne Fault Zone (MFZ). A few sites in the north of the massif present an E–W orientation, sub-parallel to the NASZ. These observations suggest that the orientation of the main productive fault zones in the Armorican Massif may be controlled by regional tectonic events.

The roles of regional and local stress tensor orientations with respect to the fracture permeability have been described (Barton et al. 1995; Henriksen and Braathen 2005; Mattila and Tammisto 2012; St. Clair et al. 2015). It is commonly stated that fractures and faults aligned subparallel to the orientation of the principal compressive stress σ_1 and are more likely to be open, and consequently more permeable, than fractures perpendicular to σ_1 . Mazabraud et al. (2004) showed from a compilation of seismological data that the maximum horizontal stress is oriented N175°E in the eastern part of the Armorican Massif and N130°E in the south-western part (Fig. 1). The fault zones that have been identified in this study show good agreement with the orientations of σ_1 deduced

from Mazabraud et al. (2004) for the area; however, some sites, mainly located in the northern part of the NASZ, appear to be perpendicular to σ_1 , which may be due to local stress tensor (re)-orientation sub-parallel to NASZ or to other local hydrogeological factors. A better knowledge of the local stress tensor orientations would help to complement this observation.

Productivity of the aquifer

In order to discuss the structural properties of the aquifer that might explain such changes in aquifer productivity and well yield, the different sites were classified into three structural categories based on geological and geophysical observations: (1) sub-vertical fault zones, (2) sub-vertical fault zones connected to a shallow reservoir and (3) sub-horizontal or gently dipping fault zones that can also be connected to an overlying reservoir. These three types of configurations typically conceptualize the different structural faulted contexts that can be found in crystalline rock basements. The shallow reservoirs could consist of either overlying weathered rocks (from regolith to shallow fractured basement), alluvial deposits, or superficial sedimentary basin connected to the fault zone.

The hydrological behaviors under pumping conditions were firstly described based on available drawdown and flow rate data recorded during pumping tests carried out on the selected sites. When the engineering offices provided time series data, the evolution of specific capacity (SC) with time of pumping was analyzed (Fig. 6, drawdown and flow-rate time series are available for 19 sites out of 23, cf. Table 1). The SC is distributed over 2 orders of magnitude, from 1 to 100 ($\text{m}^3/\text{h}/\text{m}$). It is clear that the SC decreases with pumping time—as expected from the Cooper and Jacob approximation—with transitory behaviors that greatly differ from site to site.

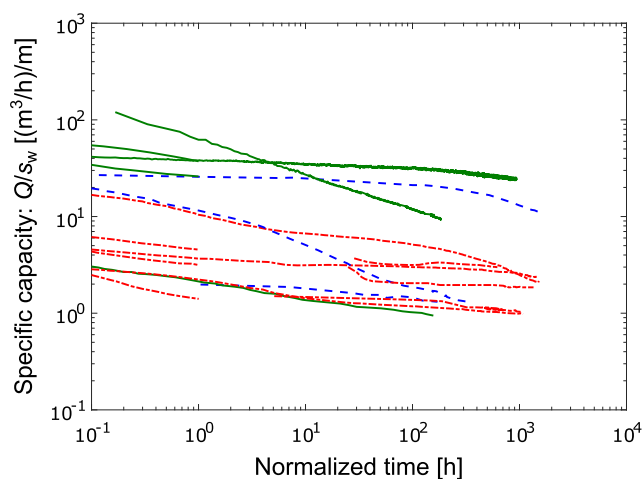


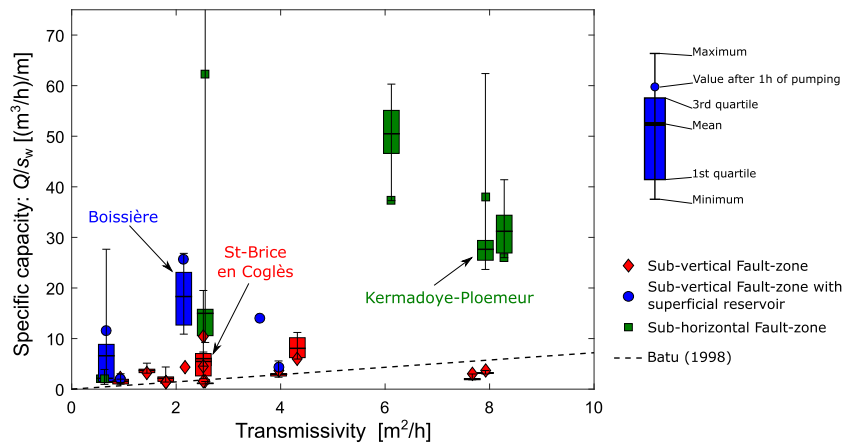
Fig. 6 Evolution of the specific capacity with pumping time for 19 sites for which time series data are available. *Red dash-dotted lines* are for sub-vertical fault zones, *blue dashed lines* are for sub-vertical fault zones connected to a shallower reservoir, and *continuous green lines* are for sub-horizontal fault zones

SC values were compared to aquifer transmissivity estimated from pumping tests (T_b) for each site (Fig. 7). In order to better evaluate the distribution of the SC parameter over the time of pumping for each site, a boxplot representation is provided when time series data of drawdown and flow rate are available (Fig. 7). The empirical relationship between T_b and SC established by Batu (1998) for confined aquifers is plotted as reference in Fig. 7 ($\text{SC} = 0.72 T_b$). No clear relationship between SC and the borehole transmissivity could be directly extracted from this plot. The model from Batu (1998) may be consistent with part of the dataset, mainly composed by the sub-vertical fault zones. Nevertheless, the estimated SC at some sites is larger than what would be expected from this empirical relationship. Such differences seem to be related to specific aquifer properties, which can enhance the productivity of the well. The presence of a shallower reservoir connected to the fault zone seems to slightly increase the productivity (blue data points in the Fig. 7); however, it is clear from Fig. 7 that three sites, for which a gently dipping fault zone has been identified, present exceptional yield properties. To discuss the general flow behaviors involved when pumping in those three main fault zone configurations, diagnostic plots—i.e. specific drawdown (Q/s_w) and its logarithmic derivative—are displayed in Fig. 8 for three characteristic sites.

The St-Brice en Coglès site is a typical example of a sub-vertical fault zone. The borehole intersects a transmissive sub-vertical fault zone at a depth of 110 m. The site is implemented in hornfels schists, in the epimetamorphism zone of a large Cadomian granitic pluton. The transmissivity of the aquifer has been estimated at $2.52 \text{ m}^2/\text{h}$ from a 2-month pumping test (Dewandel et al. 2014; Roques 2013; Roques et al. 2014a, b). Although the transmissivity of the main fault zone is large, the productivity of the well remains limited ($<10 \text{ m}^3/\text{h}/\text{m}$). Results from hydraulic testing and geochemical mixing analysis performed during the pumping test have revealed that, after a small drainage effect coming from the superficial regolith compartment at the beginning of the test (logarithmic derivative slightly decreases between 2 and 20 h in Fig. 8), the drawdown strongly increases. This increase suggests the signature of a strip aquifer response with high hydraulic property contrasts (derivative follows a slope of 0.5–1, typical of a linear response) and appears to be controlled by the less permeable reservoirs that burden the main fault zone at the end of the pumping.

An example of sub-vertical structures connected to a shallow reservoir with a strong drainage effect has been diagnosed in the Boissière site (Fig. 8). This site is located in Brioverian schists and intersects a transmissive fault zone at 80 m depth with a specific capacity of around $20 \text{ m}^3/\text{h}/\text{m}$. In its shallower part, until 20–30 m, the schists show a high density of fractures with evidence of advanced weathering. The diagnostic plot shows a strong drainage effect after 2 h of pumping coming from the shallower compartment (the logarithmic

Fig. 7 Plot of specific capacity (SC) vs. borehole transmissivity (T_b). The three main different types of conceptual structures (Fig. 6) are distinguished by a color code (*red* is sub-vertical fault, *blue* is sub-vertical fault connected to superficial reservoir, and *green* is gently dipping fault). The *dashed line* is the relationship between T and SC defined by Batu (1998) for confined aquifers



derivative is close to zero between 3 and 20 h of pumping). The drawdown is next followed by the influence of the fault zone as similarly observed in the St-Brice en Coglès site. Traou Guern site also enters in this structural configuration (note that the drawdown evolution during the pumping test is not available for this site). The site is located in an EW collapsed basin made of Brioverian schist covered by Pleistocene sandy formations 40 to 50 m thick. The boreholes intersect a sub-vertical fault zone that provides a mean flow rate of 100 m³/h from airlift measurements and a specific capacity of about 15 (m³/h)/m.

Five sub-horizontal fault zones have been identified in this study area and provide higher productivity than most other fault zones (green data points in Fig. 7). The Kermadoye-Ploemeur site is a typical example of a productive sub-horizontal fault zone. This site has been described through interdisciplinary research projects conducted over the last 15 years (Le Borgne et al. 2006; Leray et al. 2013; Ruelleu et al. 2010). The site is implemented at the contact zone between granite and micaschists, gently dipping toward the north. This contact zone has been described as the main recharge flow path of the pumping site (Leray et al. 2013). The average specific capacity for the Kermadoye-Ploemeur site is around 30 (m³/h)/m, one of the highest values identified in this study (Fig. 7). The diagnostic of the pumping test shows a typical response of radial flow in the confined aquifer both at the beginning and at the end of the pumping; the logarithmic derivative is constant until 60 h of pumping and again from 300 h to the end of the test (40 days). Those two plateaus of the logarithmic derivative of the specific drawdown are separated by a transition period indicating the influence of transmissivity-contrasted boundaries. This diagnostic highlights that, for the later times of the pumping, infinite radial flow is involved, controlled by the permeable horizontal contact zone draining the overlying reservoir (Leray et al. 2013).

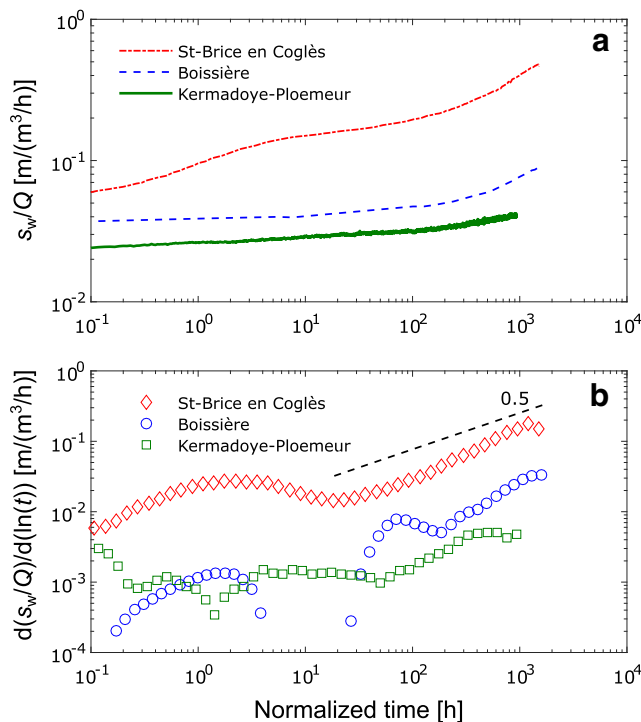


Fig. 8 Diagnostic plot of **a** specific drawdown and **b** its logarithmic derivative, of three pumping tests characteristic of the conceptual models identified in this study. Time has been normalized according to the variation of flow rate involved during the test (Bourdet and Ayoub 1989)

Discussion

Crystalline rocks are generally described as poor reservoirs with low hydrogeological properties. Groundwater resources are classically prospected in the first tens of meters of the basement where sheeting joints—and in some regions weathering processes—are more likely to develop a secondary permeability. Those aquifers generally provide low yielding but sufficient hydraulic properties for local needs (Dewandel et al. 2006; Taylor and Howard 1999). This study demonstrates that more significant hydraulic properties and groundwater resources may be found in geological structures affected

by major fault zones. In the following, the geological and hydrological conditions, which may control high-yield groundwater resources in crystalline rocks, are discussed.

Fault-zone hydrogeology in crystalline media

Exceptional values of borehole and fracture transmissivities were identified in this study. Although the number of observations decreases with depth, the average transmissivity does not present significant variation with depth, at least in the range investigated by this study (0–160 m below regolith). It demonstrates that, locally, fault zones can considerably enhance the hydraulic properties of the crystalline rocks. Faulting induces the development of a significant permeable fractured reservoir within the damaged zone, parallel to the fault plane, which can drive and store groundwater at depth (Bense et al. 2013). This dataset also suggests that fracture transmissivity is poorly influenced by the vertical component of the stress tensor for the depth range considered in this study (0–200 m). Although the fracture density slightly decreases with depth, the capacity of those fractures to conduct water seems to be constant. The good correlation between the orientation of the lineaments and the orientation of the maximum contemporary compressive stress shows that lineaments that are parallel to σ_1 are more likely to be reactivated and develop transmissive fractures. This is further evidence that a good understanding of the contemporary stress field is a critical aspect when estimating groundwater resources availability in crystalline rock.

Lithotype does not seem to influence fracture transmissivity. Although most of the investigated sites are implemented in schists, the wells located in the other lithotypes display similar fracture transmissivities. Consequently, there is no direct evidence of mechanical or mineralogical properties specific to these different lithotypes—such as the presence of foliation in the case of schist or dissolution/precipitation processes of specific mineral phases—that might influence the hydraulic properties of the fault zones in this context.

Weathering processes may also have locally influenced the hydraulic properties of the fault zones as a secondary process. For instance, the Armorican Massif was subject to arid to semi-arid climates from Eocene to Oligocene, which induced different weathering phases of the basement (Bessin et al. 2015; Guillocheau et al. 2003). The outcropping parts of the fault zones often present deeper weathering, following the fault zone orientation and dip, compared to the surrounding protolith. Supergene weathering may develop deeper weathering profiles along fault zones which constitutes preferential flow paths to meteoric water infiltration along existing opened fractures (Dewandel et al. 2011; Olesen and Dehls 2007; Place et al. 2015). This weathered unit may locally increase the storage capacity of the fault zone, by increasing the porosity in its outcropping parts.

Structure and productivity of fault zones

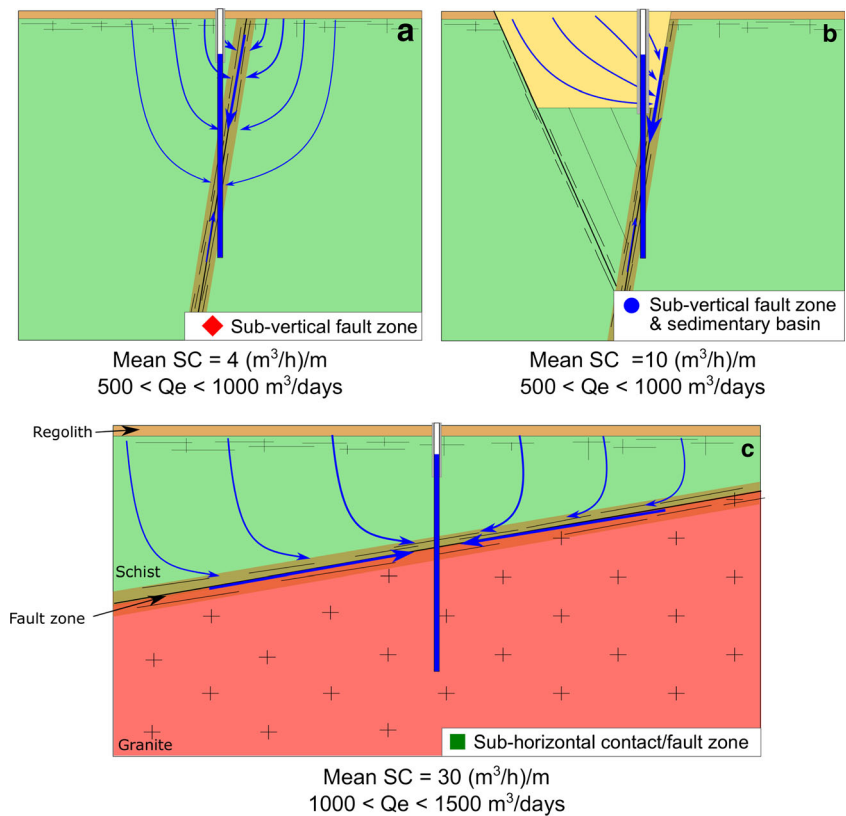
It has been shown by local field studies and numerical simulations that, apart from displaying high transmissivity, fault zones need to be connected with significant storage reservoirs to ensure long-term groundwater resources (Banks et al. 2002; Folch and Mas-Pla 2008; Leray et al. 2013; Neves and Morales 2006; Rafini and Larocque 2012; Roques et al. 2014b; Ruelleu et al. 2010). Studies have highlighted the role played by (1) the superficial fractured and weathered reservoir to feed the deeper faulted bedrock, and/or (2) the matrix pore water stored within the adjacent protolith. Thus, in addition to high transmissivity, the geometrical properties of fault zones greatly control the productivity of the aquifer; the three major structural features encountered are illustrated in Fig. 9, which conceptualizes the flow conditions involved in such a compartmented medium.

Sub-vertical fault zones were the most frequently encountered configuration in this study area. They represent about 60 % of the groundwater sites analyzed (Figs. 7 and 9). This structural case displays the lowest specific capacity. Although transmissivity and airlift flow rate can be relatively high, the specific capacity for these sub-vertical structures remains limited compared to the two other geological settings. This lower yield can be related to the restricted recharge area induced by the pumping, directly resulting from the verticality of the permeable fault zone. Sub-vertical fault zones have low storage capacity, narrow recharge area and consequently low yield when not associated with a storage reservoir (Leray et al. 2013; Roques et al. 2014b).

Figure 7 suggests that higher yields (higher SC) are related to fault zones connected with overlaying storage reservoirs and/or when the drainage basin has a greater influence (blue and green data points and box plots on Fig. 7). The high diffusivity of the fault zone can lead to a fast pressure transfer to the overlaying reservoirs. This preferential down-flow may compensate for the low or moderate storativity of the fault zone and may increase well productivity. In such a case, the fault zone optimizes drainage of the shallower reservoir along the entire length of the fault; however, the productivity will depend on the storativity of the shallower connected reservoir. Pumping test diagnoses have revealed drainage flow from the shallower fractured/weathered unit during the short time of the test (a few hours to a few days) which, in the absence of recharge, can lead to critically smaller productivity for long-term pumping operation.

Gently dipping fault zones are enhancing the aquifer productivity. As seen in the Kermadocye-Ploemeur site, pumping within a sub-horizontal permeable fault zone or contact zone induces dominant radial flow conditions. This, in turn, allows for development of a more efficient capture zone around the pumping well that can eventually drain the overlying permeable compartments and increase the well yield in the long term.

Fig. 9 Hydrogeological conceptual models of fault-zone aquifers under pumping conditions: **a** sub-vertical fault zone with limited storage reservoir, **b** sub-vertical fault zone connected to a sub-surface storage reservoir (sedimentary basin) and **c** sub-horizontal geological contact zone or fault zone. *Blue arrows* represent the main streamlines induced by pumping in a well that intersects the main fault zone. *Green and red areas* represent different lithological units. Average specific capacity (SC ; Q/s) and the range of exploitation flow rates (Q_e) are displayed for each model



(Leray et al. 2013; Ruelleu et al. 2010). Gently dipping fault and contact zones provide sustainable conditions for groundwater abstraction in the crystalline basement. The Kermadoc-Ploemeur site has been exploited for water supply since 1991 at a pumping rate of about 3,000 m³/day (1,000,000 m³/year).

This study shows that fault zones may provide exceptional groundwater resources in crystalline rocks. When permeable, these structures provide a much higher productivity than the one expected in the shallower sub-surface fractured/weathered compartment and may offer substantial resources for water supply of small cities of a few thousands inhabitants. However, fault zones may also be impervious or poorly productive in other structural settings. The identification of permeable fault zones through conventional prospection techniques (i.e. lineament analysis, geological and geophysical investigations) remains the main challenge, particularly in the case of sub-horizontal permeable structures.

Conclusions

Although restricted to the Armorican Massif, this study opens up new perspectives for the understanding of high-yield resources in crystalline basement. In particular, it allows establishing links between structural and hydrogeological

environments that may control the groundwater productivity of fault zones:

1. High-yield resources are controlled by the presence of a main transmissive fault zone. High value hydraulic properties can be encountered at relatively great depth. Vertical stress seems to have only a limited effect on hydraulic properties since the fracture transmissivity encountered does not indicate any decrease with depth, at least in the depth range considered (0–200 m).
2. The orientation of fault zones in such high-yield contexts shows good agreement with the direction expected from the stress tensor at the regional scale. The in-situ stress field plays a critical role to enhance yield properties of crystalline basement. Nevertheless, this is not clear if the stress tensor is still maintaining open fractures and fault zones parallel to the main stress component, in a similar way to what has been shown by previous works at the borehole scale (Barton et al. 1995; Henriksen and Braathen 2005; Mattila and Tammisto 2012), or if this is due to large-scale inherited structures. Further investigations are necessary to describe this relationship.
3. Aquifer productivity was found to be highly variable and to exhibit exceptional values for crystalline aquifers. The productivity of sub-vertical fault zones not connected to a superficial reservoir seems to be in any case limited. Gently dipping fault zones and/or the presence of

superficial reservoirs connected to the fault zone greatly enhance aquifer productivity. Although challenging to identify through conventional prospection techniques, a gently dipping fault zone draining overlying reservoirs remains the more productive aquifer configuration.

Acknowledgements Some of the data are freely available from the French Water Agency (Agence de l'eau Loire Bretagne 2016) and the BRGM databases (French Geological Survey, BRGM 2016). Most funding came from the CASPAR project in collaboration with OSUR and BRGM and co-funded by the European Regional Development Funding (FEDER), the Regional Council of French Brittany, the French Water Agency of Loire-Brittany (AELB), the Department of Ile-et-Vilaine, and the French Ministry for Education and Research. We also wish to thank the European INTERREG IV project CLIMAWAT and the network of hydrogeological research sites H+ (SOERE H+) which provided some of the data. We are grateful to Yvon Georget, Gilles Lucas and Philippe Bardy for sharing with us their knowledge regarding the sites. Diana Warwick is also warmly acknowledged for her detailed English editing. The authors greatly appreciate constructive remarks from the editor Jean-Michel Lemieux, the associate editor, and the two anonymous reviewers, which considerably improved the quality of the manuscript.

References

- Amiotte Suchet P, Probst J-L, Ludwig W (2003) Worldwide distribution of continental rock lithology: implications for the atmospheric/soil CO₂ uptake by continental weathering and alkalinity river transport to the oceans. *Glob Biogeochem Cycles* 17:1–13. doi:10.1029/2002GB001891
- Anderson RS (2015) Pinched topography initiates the critical zone. *Science* 350(6260):506–507. doi:10.1126/science.aad2266
- Ayraud V, Aquilina L, Labasque T, Pauwels H, Molenat J, Pierson-Wickmann A-C, Durand V, Bour O, Tarits C, Le Corre P (2008) Compartmentalization of physical and chemical properties in hard-rock aquifers deduced from chemical and groundwater age analyses. *Appl Geochem* 23:2686–2707. doi:10.1016/j.apgeochem.2008.06.001
- Ballèvre M, Bosse V, Ducassou C, Pitra P (2009) Palaeozoic history of the Armorican Massif: models for the tectonic evolution of the suture zones. *Compt Rendus Geosci* 341:174–201. doi:10.1016/j.crte.2008.11.009
- Banks D (1998) Predicting the probability distribution of yield from multiple boreholes in crystalline bedrock. *Ground Water* 36:269–274. doi:10.1111/j.1745-6584.1998.tb01092.x
- Banks D, Robins NS, Robins N (2002) An introduction to groundwater in crystalline bedrock. *Norges Geologiske Undersøkelse, Trondheim, Norway*
- Banks EW, Simmons CT, Love AJ, Cranswick R, Werner AD, Bestland E a, Wood M, Wilson T (2009) Fractured bedrock and saprolite hydrogeologic controls on groundwater/surface-water interaction: a conceptual model (Australia). *Hydrogeol J* 17:1969–1989. doi:10.1007/s10040-009-0490-7
- Barton C, Zoback M, Moos D (1995) Fluid flow along potentially active faults in crystalline rock. *Geology* 23:683–686. doi:10.1130/0091-7613(1995)023<0683:FFAPAF>2.3.CO;2
- Batu V (1998) *Aquifer hydraulics: a comprehensive guide to hydrogeologic data analysis*. Wiley, Chichester, UK, 752 pp
- Bense VF, Gleeson T, Loveless SE, Bour O, Scibek J (2013) Fault zone hydrogeology. *Earth Sci Rev* 127:171–192. doi:10.1016/j.earscirev.2013.09.008
- Berkowitz B (2002) Characterizing flow and transport in fractured geological media: a review. *Adv Water Resour* 25:861–884. doi:10.1016/S0309-1708(02)00042-8
- Bessin P, Guillocheau F, Robin C, Schroëtter JM, Bauer H (2015) Planation surfaces of the Armorican Massif (western France): denudation chronology of a Mesozoic land surface twice exhumed in response to relative crustal movements between Iberia and Eurasia. *Geomorphology* 233:75–91. doi:10.1016/j.geomorph.2014.09.026
- Blatt H, Jones R (1975) Proportions of exposed igneous, metamorphic, and sedimentary rocks. *Geol Soc Am Bull* 86:1085–1088. doi:10.1130/0016-7606(1975)86<1085:POEIMA>2.0.CO;2
- Bonnet S, Guillocheau F, Brun J-P, Van Den Driessche J (2000) Large-scale relief development related to Quaternary tectonic uplift of a Proterozoic-Paleozoic basement: the Armorican Massif, NW France. *J Geophys Res* 105:19273–19288. doi:10.1029/2000JB900142
- Bourdet D, Ayoub J (1989) Use of pressure derivative in well test interpretation. *SPE Form Eval* 4:293–302
- Boutt DF, Diggins P, Mabee S (2010) A field study (Massachusetts, USA) of the factors controlling the depth of groundwater flow systems in crystalline fractured-rock terrain. *Hydrogeol J* 18:1839–1854. doi:10.1007/s10040-010-0640-y
- Butler JJ, Liu WZ (1991) Pumping tests in non-uniform aquifers: the linear strip case. *J Hydrol* 128:69–99. doi:10.1016/0022-1694(91)90132-2
- Caine J, Evans J, Forster C (1996) Fault zone architecture and permeability structure. *Geology* 24:1025–1028. doi:10.1130/0091-7613(1996)024<1025
- Chantraine J, Egal E, Thiéblemont D, Le Goff E, Guerrot C, Ballèvre M, Guennoc P (2001) The Cadomian active margin (North Armorican Massif, France): a segment of the North Atlantic Panafrikan belt. *Tectonophysics* 331:1–18. doi:10.1016/S0040-1951(00)00233-X
- Chilton PJ, Foster SDS (1995) Hydrogeological characterization and water-supply potential of basement aquifers in tropical Africa. *Hydrogeol J* 3:36–49. doi:10.1007/s100400050061
- Dewandel B, Lachassagne P, Wyns R, Maréchal JC, Krishnamurthy NS (2006) A generalized 3-D geological and hydrogeological conceptual model of granite aquifers controlled by single or multiphase weathering. *J Hydrol* 330:260–284. doi:10.1016/j.jhydrol.2006.03.026
- Dewandel B, Lachassagne P, Zaidi FK, Chandra S (2011) A conceptual hydrodynamic model of a geological discontinuity in hard rock aquifers: example of a quartz reef in granitic terrain in South India. *J Hydrol* 405:474–487. doi:10.1016/j.jhydrol.2011.05.050
- Dewandel B, Maréchal JC, Bour O, Ladouche B, Ahmed S, Chandra S, Pauwels H (2012) Upscaling and regionalizing hydraulic conductivity and effective porosity at watershed scale in deeply weathered crystalline aquifers. *J Hydrol* 416–417:83–97. doi:10.1016/j.jhydrol.2011.11.038
- Dewandel B, Aunay B, Maréchal JC, Roques C, Bour O, Mouglin B, Aquilina L (2014) Analytical solutions for analysing pumping tests in a sub-vertical and anisotropic fault zone draining shallow aquifers. *J Hydrol* 509:115–131. doi:10.1016/j.jhydrol.2013.11.014
- Folch A, Mas-Pla J (2008) Hydrogeological interactions between fault zones and alluvial aquifers in regional flow systems. *Hydrol Process* 22:3476–3487. doi:10.1002/hyp.6956
- Gleeson T, Novakowski K (2009) Identifying watershed-scale barriers to groundwater flow: lineaments in the Canadian shield. *Geol Soc Am Bull* 121:333–347. doi:10.1130/B26241.1
- Gleeson T, Smith L, Moosdorf N, Hartmann J, Dürr HH, Manning AH, van Beek LPH, Jellinek AM (2011) Mapping permeability over the surface of the Earth. *Geophys Res Lett* 38, L02401. doi:10.1029/2010GL045565
- Gleeson T, Wada Y, Bierkens MFP, van Beek LPH (2012) Water balance of global aquifers revealed by groundwater footprint. *Nature* 488:197–200. doi:10.1038/nature11295
- Guihéneuf N, Boisson A, Bour O, Dewandel B, Perrin J, Dausse A, Viossanges M, Chandra S, Ahmed S, Maréchal JC (2014)

- Groundwater flows in weathered crystalline rocks: impact of piezometric variations and depth-dependent fracture connectivity. *J Hydrol*. doi:10.1016/j.jhydrol.2014.01.061
- Guillocheau F, Brault N, Thomas E, Barbarand J, Bonnet S, Bourquin S, Estéoule-Choux J, Guennoc P, Menier D, Néraudeau D, Proust J, Wyns R (2003) Histoire géologique du Massif Armoricain depuis 140 MA (Crétacé-Actuel) [Geological History of the Armorican Massif since 140 My (Cretaceous-Current)]. *Bull Information Géol Bassin Paris* 40:13–28
- Hencher SR, Lee SG, Carter TG, Richards LR (2011) Sheeting joints: characterisation, shear strength and engineering. *Rock Mech Rock Eng* 44:1–22. doi:10.1007/s00603-010-0100-y
- Henriksen H (2003) The role of some regional factors in the assessment of well yields from hard-rock aquifers of Fennoscandia. *Hydrogeol J* 11:628–645. doi:10.1007/s10040-003-0277-1
- Henriksen H, Braathen A (2005) Effects of fracture lineaments and in-situ rock stresses on groundwater flow in hard rocks: a case study from Sunnfjord, western Norway. *Hydrogeol J* 14:444–461. doi:10.1007/s10040-005-0444-7
- Kabala ZJ (1994) Measuring distributions of hydraulic conductivity and specific storativity by the double flowmeter test. *Water Resour Res* 30:685–690. doi:10.1029/93WR03104
- Le Borgne T, Bour O, Paillet F, Caudal J (2006) Assessment of preferential flow path connectivity and hydraulic properties at single-borehole and cross-borehole scales in a fractured aquifer. *J Hydrol* 328:347–359. doi:10.1016/j.jhydrol.2005.12.029
- Le Borgne T, De Dreuzy JR, Davy P, Bour O (2007) Characterization of the velocity field organization in heterogeneous media by conditional correlation. *Water Resour Res* 43:1–10. doi:10.1029/2006WR004875
- Leray S, de Dreuzy J-R, Bour O, Bresciani E (2013) Numerical modeling of the productivity of vertical to shallowly dipping fractured zones in crystalline rocks. *J Hydrol* 481:64–75. doi:10.1016/j.jhydrol.2012.12.014
- Mabee SB (1999) Factors influencing well productivity in glaciated metamorphic rocks. *Ground Water* 37:88–97. doi:10.1111/j.1745-6584.1999.tb00961.x
- Malgrange J, Gleeson T (2014) Shallow, old, and hydrologically insignificant fault zones in the Appalachian orogen. *J Geophys Res Solid Earth* 119:346–359. doi:10.1002/2013JB010351
- Maréchal JC, Dewandel B, Subrahmanyam K (2004) Use of hydraulic tests at different scales to characterize fracture network properties in the weathered-fractured layer of a hard rock aquifer. *Water Resour Res* 40, W11508. doi:10.1029/2004WR003137
- Mattila J, Tammisto E (2012) Stress-controlled fluid flow in fractures at the site of a potential nuclear waste repository, Finland. *Geology* 40:299–302. doi:10.1130/G32832.1
- Mazabraud Y, Béthoux N, Guilbert J, Bellier O (2004) Evidence for short-scale stress field variations within intraplate central-western France. *Geophys J Int* 160:161–178. doi:10.1111/j.1365-246X.2004.02430.x
- Mazabraud Y, Béthoux N, Deroussi S (2005) Characterisation of the seismological pattern in a slowly deforming intraplate region: central and western France. *Tectonophysics* 409:175–192. doi:10.1016/j.tecto.2005.08.021
- Meier PM, Carrera J, Sánchez-Vila X (1998) An evaluation of Jacob's method for the interpretation of pumping tests in heterogeneous formations. *Water Resour Res* 34:1011–1025. doi:10.1029/98WR00008
- Mougin B, Allier D, Blanchin R, Carn A, Courtois N, Gateau C, Putot E (2008) SILURES Bretagne (Système d'Information pour la Localisation et l'Utilisation des Ressources en Eaux Souterraines) [SILURES Bretagne (Information system for the location and use of groundwater resources in the Armorican Massif)]. Final report, BRGM/RP-56457. www.brgm.fr. Accessed July 2016
- Neves MA, Morales N (2006) Well productivity controlling factors in crystalline terrains of southeastern Brazil. *Hydrogeol J* 15:471–482. doi:10.1007/s10040-006-0112-6
- Olesen O, Dehls J (2007) Aeromagnetic mapping of deep-weathered fracture zones in the Oslo Region: a new tool for improved planning of tunnels. *Nor J Geol* 87:253–267
- Paillet FL (1998) Flow modeling and permeability estimation using borehole flow logs in heterogeneous fractured formations. *Water Resour Res* 34:997–1010. doi:10.1029/98WR00268
- Place J, Géraud Y, Diraison M, Herquel G, Edel J-B, Bano M, Le Garzic E, Walter B (2015) Structural control of weathering processes within exhumed granitoids: compartmentalisation of geophysical properties by faults and fractures. *J Struct Geol* 84:102–119. doi:10.1016/j.jsg.2015.11.011
- Rafini S, Larocque M (2012) Numerical modeling of the hydraulic signatures of horizontal and inclined faults. *Hydrogeol J* 20:337–350. doi:10.1007/s10040-011-0812-4
- Ranjram M, Gleeson T, Luijendijk E (2015) Is the permeability of crystalline rock in the shallow crust related to depth, lithology or tectonic setting? *Geofluids* 15:106–119. doi:10.1111/gfl.12098
- Razack M, Lasm T (2006) Geostatistical estimation of the transmissivity in a highly fractured metamorphic and crystalline aquifer (Mandane Region, Western Ivory Coast). *J Hydrol* 325:164–178. doi:10.1016/j.jhydrol.2005.10.014
- Renard P, Glenz D, Mejias M (2008) Understanding diagnostic plots for well-test interpretation. *Hydrogeol J* 17:589–600. doi:10.1007/s10040-008-0392-0
- Roques C (2013) Hydrogéologie des zones de faille du socle cristallin: implications en terme de ressources en eau pour le Massif Armoricain (Fault zone hydrogeology in crystalline media: implication in term of groundwater resources for the Armorican Massif). Numéro 148 des Mémoires de géosciences Rennes, Université Rennes 1, Rennes, France
- Roques C, Aquilina L, Bour O, Maréchal J-C, Dewandel B, Pauwels H, Labasque T, Vergnaud-Ayraud V, Hochreutener R (2014a) Groundwater sources and geochemical processes in a crystalline fault aquifer. *J Hydrol* 519:3110–3128. doi:10.1016/j.jhydrol.2014.10.052
- Roques C, Bour O, Aquilina L, Dewandel B, Leray S, Schroetter JM, Longuevergne L, Le Borgne T, Hochreutener R, Labasque T, Lavenant N, Vergnaud-Ayraud V, Mougin B (2014b) Hydrological behavior of a deep sub-vertical fault in crystalline basement and relationships with surrounding reservoirs. *J Hydrol* 509:42–54. doi:10.1016/j.jhydrol.2013.11.023
- Ruelleu S, Moreau F, Bour O, Gapais D, Martelet G (2010) Impact of gently dipping discontinuities on basement aquifer recharge: an example from Ploumeur (Brittany, France). *J Appl Geophys* 70:161–168. doi:10.1016/j.jappgeo.2009.12.007
- Seebeck H, Nicol A, Walsh JJ, Childs C, Beetham RD, Pettinga J (2014) Fluid flow in fault zones from an active rift. *J Struct Geol* 62:52–64. doi:10.1016/j.jsg.2014.01.008
- Singhal B, Gupta R (2010) Applied hydrogeology of fractured rocks, 2nd edn. Springer, Heidelberg, Germany. doi:10.1007/978-90-481-8799-7
- Srivastav SK, Lubczynski MW, Biyani AK (2007) Upscaling of transmissivity, derived from specific capacity: a hydrogeomorphological approach applied to the Doon Valley aquifer system in India. *Hydrogeol J* 15:1251–1264. doi:10.1007/s10040-007-0207-8
- St. Clair J, Moon S, Holbrook WS, Perron JT, Riebe CS, Martel SJ, Carr B, Harman C, Singha K, Richter DD (2015) Geophysical imaging reveals topographic stress control of bedrock weathering. *Science* 350(6260):534–538. doi:10.1126/science.aab2210
- Stober I, Bucher K (2006) Hydraulic properties of the crystalline basement. *Hydrogeol J* 15:213–224. doi:10.1007/s10040-006-0094-4
- Stober I, Bucher K (2014) Hydraulic conductivity of fractured upper crust: insights from hydraulic tests in boreholes and fluid-rock interaction in crystalline basement rocks. *Geofluids* 15(2015):161–178. doi:10.1111/gfl.12104
- Taylor RG, Howard KWF (1999) Lithological evidence for the evolution of weathered mantles in Uganda by tectonically controlled cycles of

- deep weathering and stripping. *CATENA* 35:65–94. doi:[10.1016/S0341-8162\(98\)00118-0](https://doi.org/10.1016/S0341-8162(98)00118-0)
- Taylor R, Howard K (2002) A tectono-geomorphic model of the hydrogeology of deeply weathered crystalline rock: evidence from Uganda. *Hydrogeol J* 8:279–294. doi:[10.1007/s100400000069](https://doi.org/10.1007/s100400000069)
- Theis CV (1935) The relation between the lowering of the Piezometric surface and the rate and duration of discharge of a well using ground-water storage. *Trans Am Geophys Union* 16:519. doi:[10.1029/TR016i002p00519](https://doi.org/10.1029/TR016i002p00519)
- Van Vliet-Lanoë B, Bonnet S, Hallegouët M, Laurent M (1997) Neotectonic and seismic activity in the Armorican and Cornubian Massifs: regional stress field with glacio-isostatic influence? *J Geodyn* 24(1–4):219–239. Retrieved from <http://www.sciencedirect.com/science/article/pii/S026437079600035X>
- Welch LA, Allen DM (2014) Hydraulic conductivity characteristics in mountains and implications for conceptualizing bed-rock groundwater flow. *Hydrogeol J*. doi:[10.1007/s10040-014-1121-5](https://doi.org/10.1007/s10040-014-1121-5)
- Wyns R, Baltassat J, Lachassagne P, Legchenko A, Vairon J (2004) Application of proton magnetic resonance soundings to groundwater reserve mapping in weathered basement rocks (Brittany, France). *Bull Soc Géol Fr* 175:21–34. doi:[10.2113/175.1.21](https://doi.org/10.2113/175.1.21)

Online database

- Agence de l'eau Loire-Bretagne (2016) French Water Agency, données prélèvement eau potable [Water supply database]. <http://www.eau-loire-bretagne.fr/>. Accessed July 2016
- BRGM (2016) Bureau de Recherches Géologiques et Minières (French Geological Survey), Infoterre database, Dossiers sur le Sous-Sol BSS [Underground database]. <http://infoterre.brgm.fr/dossiers-sur-le-sous-sol-bss>. Accessed July 2016